Steel and Composite Structures, *Vol. 18, No. 3 (2015) 565-582*
DOI: http://dx.doi.org/10.12989/scs.2015.18.3.565

Dynamic analysis and model test on steel-concrete composite beams under moving loads

Zhongming Hou [*1,2], He Xia [1], Yuanqing Wang [2], Yanling Zhang [3] and Tianshen Zhang [2]

[1] *School of Civil Engineering, Beijing Jiaotong University, Beijing 100044, China*
[2] *Department of Civil Engineering, Tsinghua University, Beijing, 100084, China*
[3] *School of Civil Engineering, Shijiazhuang Tiedao University, Shijiazhuang 050043, Hebei, China*

(*Received January 27, 2014, Revised June 11, 2014, Accepted August 21, 2014*)

Abstract. This paper is concerned with the dynamic analysis of simply-supported steel-concrete composite beams under moving loads. Considering the interface slip between steel girder and concrete slab, the governing motion equations are derived from the direct balanced method. By variable separation approach, the analytical solution of natural frequencies and mode shapes are obtained, as well as the orthogonal conditions. Then the dynamic responses of the composite beam under moving loads are analyzed, and compared with the experimental results. The analysis results show that the governing motion equations become more complicated when interface slip is taken into account, and the dynamic behaviors are significantly influenced by the shear connection stiffness. In the dynamic calculation of composite beams, the global stiffness should not be reduced as the same factor to all orders, but as different ones according to the dynamic stiffness reduction factor (DSRF), to which should be paid more attention in calculation, design and experiment, or else great deviation is inevitable.

Keywords: steel-concrete composite beam; dynamic characteristics; natural frequency; orthogonal condition; moving loads; analytical solution; model test

1. Introduction

The steel-concrete composite beams (short for composite beam herein) are composed of concrete slab and steel girder, which are connected by shear connectors (e.g., headed studs), as shown in Fig. 1. Taking full advantage of material properties of the compressive concrete slab and the tensile steel girder, the composite beams possess excellent mechanical performance, diversified format and convenient construction, which are widely adopted in highway and railway bridges. For bridges with short and medium spans, especially for spans of 60 m to 80 m, the construction cost of composite beams is 18% less than that of the concrete bridges, and have significant advantages in comprehensive benefits (Taly 1998). In Europe and America, almost all the short bridges with the span between 25 m and 60 m are composite beams (Galambos 2000).

Nevertheless, due to the flexibility of shear connectors, interface slip will inevitably occur between the interface of concrete slab and steel girder under external loads, which affects not only

*Corresponding author, Assistant Research Fellow, Ph.D., E-mail: hou.zhong.ming@163.com

http://www.techno-press.org/?journal=scs&subpage=8 ISSN: 1229-9367 (Print), 1598-6233 (Online)

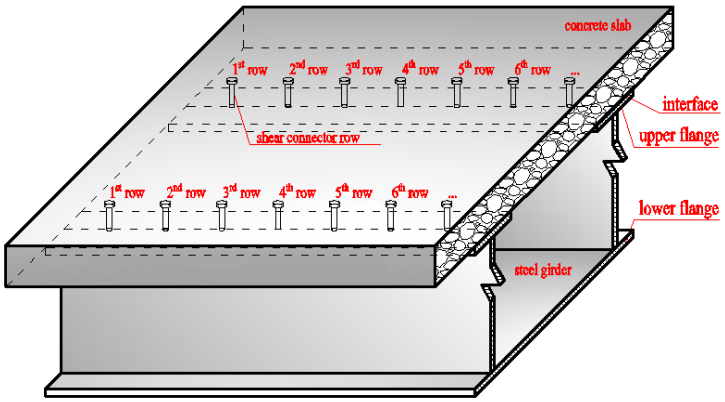

Fig. 1 Typical composite beams with shear connectors ○

the static (e.g., Zhang 2002, Kroflic *et al*. 2010), but also the dynamic behaviors of composite beams. For this reason, it shows significant differences from the beams with homogenous material (e.g., concrete beam, steel girder) (Banerjee 2001, Jiang *et al*. 2006).

The effects produced by such interface slip have been considered a lot in static calculations (e.g., Nie *et al*. 1994), but very few can be found for dynamic analyses (e.g., Biscontin *et al*. 2000, Huang and Su 2008, Kim 2009). For bridges subjected to moving loads, both the loads and the dynamic response of the beam vary with time (Xia *et al*. 2003, 2007, Esmailzadeh and Jalili 2003), which makes the dynamic equations even more complex, but references about theoretical and experimental studies of composite beams under moving loads are even far rarer.

Generally, in the published references, there are several types of concerns and methodologies for composite beams that considering interface slip.

The early method (i.e., "transformed section method") was based on elastic theory, which was first proposed by Andrews (1912). In this method, both the steel and concrete are considered as idealized elastic materials, fully connected and deformable compatibility. The concrete is transformed to the steel through the modular ratio, and then calculated based on mechanics of materials. However, the real relative slip at the interface between steel girder and concrete slab was not taken into account, which will inevitably lead to unsafe results in bearing capacity and deflection. It should be mentioned that the elastic method is only applicable to the analysis of serviceability limit state.

To avoid the calculation error caused by the elastic method, the stiffness calculation formulae were proposed, such as the "stiffness reduction factor" method (Nie *et al*. 1998) and the "combination coefficient" method (Wang *et al*. 2005), in which the effect of global stiffness degradation caused by interface slip can be taken into account. However, in the "stiffness reduction factor" method, the expression of stiffness reduction factor is not monotonic, and is restricted by the value range of connection stiffness. While in the "combination coefficient" method, which is based on the half-theory and half-experience approach, only two extreme values for the amplification coefficient are available from the connection stiffness, other values between them can only be obtained by interpolation, and it can only be used to calculate the deflection of composite beams with partial connection.

In the third type method (e.g., Nie *et al*. 1994, 1998, Wang 1998), the additional deflection

caused by interface slip are derived from the differential equation of relative slip, by which the general deflection formulae of composite beams that considered the flexible connectors were obtained. In this method, the influences of slip effect and connection degree are inclusive and some correction factors and construct restrictions are introduced to meet the requirements of calculation and engineering.

Methods based on variational principle of energy were proposed by Ranzi and Zonab (2007) and Zhang (2009). By assuming different longitudinal shape functions for the inner roof, the cantilever flanges of concrete slab and the lower plane of steel girder, and considering the relative slip of them, the analytical solutions to the deflection of the composite beams under different load distribution forms were derived. In the methods, the influences of shear deformation and shear lag are taken into account, while some coefficients are difficult to calculate.

Up to now, most of the deflection solutions for composite beams that consider interface slip are related to static theory, while those concerned with the dynamic behaviors are rarely involved.

Xu and Wu (2007) studied the static, dynamic and buckling behaviors of partial interaction composite members by taking into account the influences of rotary inertia and shear deformations, and the analytical solutions of the deflection were found for the beam with uniformly distributing load under common boundary conditions. Nie *et al*. (1998) derived a closed-form solution for the simple partial composite beam subjected to a moving load, but without damping considered. Girhammar *et al*. (2009) discussed the partial differential equations and general solutions for the deflection and internal actions and the pertaining consistent boundary conditions for composite Euler-Bernoulli members with interlayer slip subjected to general dynamic loading. Considering the rotary inertia and the shear deformation, Won *et al*. (2012) studied a damped Timoshenko beam element for the DOF-efficient forced vibration analysis of beam-like structures coated with viscoelastic damping layers, in which the complex composite section is replaced with a homogeneous one by means of the transformed section approach.

In this paper, some typical analysis models of composite beams are summarized. On this basis, the fundamental motion equations for simply-supported composite beams are derived, and the orthogonality conditions about mass, damping and stiffness matrices are obtained, as well as the "dynamic reduction factor" is discussed. Based on the modal superposition method, the solution to the dynamic response for composite beams under moving loads is proposed. The relevant dynamic experiments are carried out, and some results are compared with the numerical results.

2. Fundamental analytical model and governing equations

To consider the effect of shear connectors, an infinitesimal element of composite beam is established, which is composed of two sub-beams, a concrete slab and a steel girder, as shown in Fig. 2.

Based on considerable established research results (e.g., Biscontin *et al*. 2000, Dilena and Morassi 2003, Huang and Su 2008), some reasonable assumptions involved in the model are as follows:

(1) There is no separation due to the lift of concrete slab from steel girder;
(2) Both the concrete slab and steel girder are treated as Euler-Bernoulli beams;
(3) The shear forces borne by the connectors distribute evenly along the beams;
(4) The binding force on the interface of concrete slab and steel girder is ignored;
(5) The load is treated as concentrated force.

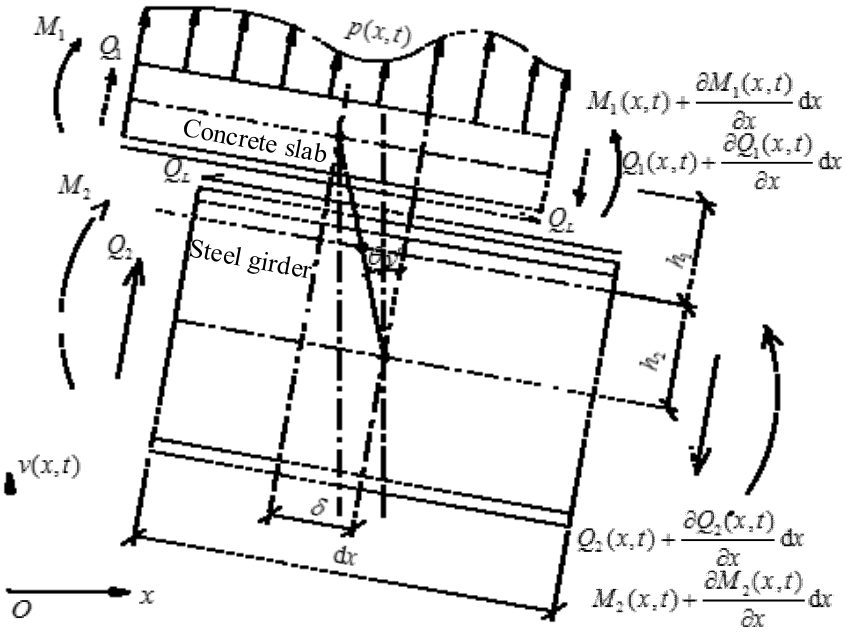

Fig. 2 Mechanical schematic diagram of composite beams

2.1 Infinitesimal element balanced equation

An infinitesimal element of dx segment is studied, in which the shear force on the interface can be expressed as $Q_L(x) = K_S\delta dx$, where K_S is the shear stiffness of the connector per unit length, and δ is the relative slip in the range of dx, with the subscripts 1 and 2 denoting the concrete slab and the steel girder, respectively.

(1) Equilibrium equations of vertical forces

Considering the vertical force equilibrium of the sub-beams, the equilibrium equation for the vertical force of the infinitesimal element can be written as

$$\frac{\partial Q(x,t)}{\partial x} = p(x,t) - m(x)\frac{\partial^2 v(x,t)}{\partial t^2} - c(x)\frac{\partial v(x,t)}{\partial t} \tag{1}$$

where $v(x, t)$ is the vertical displacement; $Q(x, t)$, $p(x, t)$, $m(x)$ and $c(x)$ are the shear force, vertical force, mass and damping factors subjected by unit length of beam, respectively.

(2) Equilibrium equations of moments

By summation of the bending moments at the right side of the neutral axes for the two sub-beams, the vertical moment equilibrium equations for the infinitesimal element of the composite beam can be obtained as

$$\frac{\partial M(x,t)}{\partial x} = Q(x,t) + K_S h\delta \tag{2}$$

where $M(x, t)$ is the moment borne by the element, and h is the distance between the neutral axes of concrete slab and steel girder. Addtionally, the minterm is neglected in this equation

(3) Displacement compatibility equations

Suppose the vertical displacement $v(x, t)$ causes a longitudinal relative slip δ and a rotation angle v' at the interface, and the corresponding relative rotation angle of the normal line of the neutral axes is θ, it can be seen from Fig. 2 that

$$\delta = (\theta + v')h \tag{3}$$

Apparently, for the infinitesimal element dx, a relational expression can be expressed as

$$K_S h^2(\theta + v') = (EI)_C \theta'' \tag{4}$$

in which the left term is the moment caused by the slip δ, and the right term is the moment caused by the rotational angle θ.

(4) Motion equation of composite beams

From Eqs. (1) to (4), the motion equations of a straight composite beam with uniform section that considering the relative slip are obtained. If $m(x)$ and $c(x)$ are treated as constants $\overline{m}$ and $\overline{c}$ respectively, the motion equation solved by the method of variables separation are obtained as

$$\frac{\mathrm{d}^6\phi(x)}{\mathrm{d}x^6} - \frac{K_S h^2 (EI)_F}{(EI)_C (EI)_B}\frac{\mathrm{d}^4\phi(x)}{\mathrm{d}x^4} - \frac{\overline{m}\omega^2}{(EI)_B}\frac{\mathrm{d}^2\phi(x)}{\mathrm{d}x^2} + \frac{K_S h^2 \overline{m}\omega^2\phi(x)}{(EI)_C (EI)_B} = 0 \tag{5}$$

where $\omega = \sqrt{k^*/m^*}$ represents the circular frequency of the system, in which $k^* = \frac{\mathrm{d}^6\phi(x)}{\mathrm{d}x^6} - \frac{K_S h^2 (EI)_F}{(EI)_C (EI)_B}\frac{\mathrm{d}^4\phi(x)}{\mathrm{d}x^4}$ and $m^* = \frac{\overline{m}}{(EI)_B}\frac{\mathrm{d}^2\phi(x)}{\mathrm{d}x^2} + \frac{K_S h^2 \overline{m}\phi(x)}{(EI)_C (EI)_B}$ are the general stiffness and mass of the system, respectively;

$v(x, t) = \phi(x)\cdot q(t)$ represents the vertical displacement of $v(x, t)$ occurring at x, in which $\phi(x)$ is the mode shape and $q(t)$ the amplitude varying with time;

$(EI)_B = E_1 I_1 + E_2 I_2$ represents the sum of bending stiffness for the concrete slab and steel girder around their respective neutral axes;

$(EI)_C = E_1 A_1 h_1^2 + E_2 A_2 h_2^2$ represents the bending stiffness around the neutral axis of the composite beam. It can be seen that the expression is similar to the conventional beams, except the expression of global stiffness.

$(EI)_F = (EI)_C + (EI)_B$ represents the stiffness of the composite beam when K_S is infinite, i.e., in the case without interface slip.

(5) Solutions to the motion equation

If λ and $\phi(x)$ are regarded as the eigenvalue and eigenfunction of Eq. (5), the solution can be expressed as

$$\phi(x) = A\sinh\lambda_1 + B\cosh\lambda_1 x + C\sinh\lambda_2 x + D\cosh\lambda_2 x + E\sinh\lambda_3 x + F\cosh\lambda_3 x \tag{6}$$

where λ_i (i = 1, 2, 3,..., 6) is the roots of the characteristic equation for Eq. (6); The coefficients A, B, ……, F can be obtained using the corresponding boundary conditions.

For a simply-supported composite beam, the mode shape can be expressed as $\phi_n(x) = \sin(n\pi x / L)$, and the circular frequency for the beam is obtained as

$$\omega_n^2 = \gamma_n^2 \frac{(n\pi)^4 (EI)_{\mathrm{F}}}{\overline{m} L^4} \tag{7}$$

where $\gamma_n^2 = \dfrac{1+\beta+(n\pi)^2\alpha}{(1+\beta)[1+(n\pi)^2\alpha]}$, $\alpha = \dfrac{(EI)_{\mathrm{C}}}{K_{\mathrm{S}} h^2 L (EI)_{\mathrm{C}}}$, $\beta = (EI)_{\mathrm{C}}(EI)_{\mathrm{B}}$.

With regard to a conventional beam with homogenous material, K_{S} tends to be infinite, i.e., α ends to be 0 and γ_n^2 tends to be 1, as a result

$$\omega_{n,\mathrm{F}} = \frac{(n\pi)^2}{L^2} \sqrt{\frac{(EI)_{\mathrm{F}}}{\overline{m}}} \tag{8}$$

Eq. (8) has the same form with conventional straight beams, and $(EI)_{\mathrm{F}}$ can be deemed as the global stiffness of composite beams without taking account of slip, thus we have

$$\omega_n = \gamma_n \omega_{n,\mathrm{F}} \tag{9}$$

$$(EI)_{\mathrm{eq}} = \gamma_n^2 (EI)_{\mathrm{F}} \tag{10}$$

where $(EI)_{\mathrm{eq}}$ represents the equivalent stiffness of composite beams.

From Eqs. (7) and (8) we can see that the vertical natural frequencies will decrease when the interface slip is considered, thus γ_n^2 reflects the dynamic stiffness of the composite beam, which can be regarded as "Dynamic stiffness reduction factor (DSRF)" of the n^{th} order, and γ_n is the "Frequency reduction factor (FRF)".

2.2 Orthogonality conditions of the mode shape

For the n^{th} mode shape, Eq. (5) can be rewritten as

$$\frac{\mathrm{d}^6\phi_n(x)}{\mathrm{d}x^6} - \frac{K_{\mathrm{S}} h^2 (EI)_{\mathrm{F}}}{(EI)_{\mathrm{C}}(EI)_{\mathrm{B}}} \frac{\mathrm{d}^4\phi_n(x)}{\mathrm{d}x^4} - \frac{\overline{m}\omega^2}{(EI)_{\mathrm{B}}} \frac{\mathrm{d}^2\phi_n(x)}{\mathrm{d}x^2} + \frac{K_{\mathrm{S}} h^2 \overline{m}\omega^2}{(EI)_{\mathrm{C}}(EI)_{\mathrm{B}}} = \phi_n(x) = 0 \tag{11}$$

By multiplying $\phi_m(x)$ to both sides of the equation and integrating along the x-axis, the orthogonality of Eq. (11) is investigated. After conducting partial integration, we obtain

$$\int_0^L \left[\frac{\mathrm{d}^6\phi_n(x)}{\mathrm{d}x^6} - \frac{K_{\mathrm{S}} h^2 (EI)_{\mathrm{F}}}{(EI)_{\mathrm{C}}(EI)_{\mathrm{B}}} \frac{\mathrm{d}^4\phi_n(x)}{\mathrm{d}x^4} - \frac{\overline{m}\omega^2}{(EI)_{\mathrm{B}}} \frac{\mathrm{d}^2\phi_n(x)}{\mathrm{d}x^2} + \frac{K_{\mathrm{S}} h^2 \overline{m}\omega^2 \phi_n(x)}{(EI)_{\mathrm{C}}(EI)_{\mathrm{B}}} \right] \phi_m(x)\mathrm{d}x \tag{12}$$

↓

$$
\begin{aligned}
&\uparrow \\
&= \left\{ \left[\phi_n^{(5)}(x) - \frac{K_S h^2 (EI)_F}{(EI)_C (EI)_B} \phi_n'''(x) - \frac{\overline{m}\omega_n^2}{(EI)_B} \phi_n'(x) \right] \phi_m(x) \right\} \Big|_0^L \\
&\quad + \left\{ \left[\phi_n^{(4)}(x) - \frac{K_S h^2 (EI)_F}{(EI)_C (EI)_B} \phi_n''(x) \right] \phi_m'(x) \right\} \Big|_0^L \\
&\quad + \phi_m''(x)\phi_n'''(x)\Big|_0^L - \int_0^L \phi_n'''(x)\phi_m'''(x)\mathrm{d}x - \int_0^L \frac{K_S h^2 (EI)_F}{(EI)_C (EI)_B} \phi_m''(x)\phi_n''(x)\mathrm{d}x \\
&\quad + \int_0^L \frac{\overline{m}\omega_n^2}{(EI)_B} \phi_m'(x)\phi_n'(x)\mathrm{d}x + \int_0^L \frac{K_S h^2 \overline{m}\omega_n^2}{(EI)_C (EI)_B} \phi_m(x)\phi_n(x)\mathrm{d}x = 0
\end{aligned} \tag{12}
$$

For a simply-supported composite beam, the first three terms at the right hand side with definite integral from 0 to L equal to zero, thus a simplified symmetric form can be obtained as

$$
\frac{\overline{m}\omega_n^2}{(EI)_B} \int_0^L \left[\phi_m'(x)\phi_n'(x) + \frac{K_S h^2}{(EI)_C} \phi_m(x)\phi_n(x) \right] \mathrm{d}x = \int_0^L \left[\phi_n'''(x)\phi_m'''(x) + \frac{K_S h^2 (EI)_F}{(EI)_C (EI)_B} \phi_m''(x)\phi_n''(x) \right] \mathrm{d}x \tag{13}
$$

Apparently, Eq. (13) is still valid when n and m are exchanged for each other due to the symmetry, we obtain

$$
\frac{\overline{m}\omega_m^2}{(EI)_B} \int_0^L \left[\phi_m'(x)\phi_n'(x) + \frac{K_S h^2}{(EI)_C} \phi_m(x)\phi_n(x) \right] \mathrm{d}x = \int_0^L \left[\phi_n'''(x)\phi_m'''(x) + \frac{K_S h^2 (EI)_F}{(EI)_C (EI)_B} \phi_m''(x)\phi_n''(x) \right] \mathrm{d}x \tag{14}
$$

Subtracting Eq. (13) from Eq. (14), we have

$$
\frac{\overline{m}(\omega_m^2 - \omega_n^2)}{(EI)_B} \int_0^L \left[\phi_m'(x)\phi_n'(x) + \frac{K_S h^2}{(EI)_C} \phi_m(x)\phi_n(x) \right] \mathrm{d}x = 0 \tag{15}
$$

For a real beam, the natural frequencies of different orders are different for each other, namely $\omega_m^2 \neq \omega_n^2$ when $m \neq n$, so the modal shapes $\phi_m(x)$ and $\phi_n(x)$ should satisfy the orthogonality conditions

$$
\frac{\overline{m}}{(EI)_B} \int_0^L \left[\phi_m'(x)\phi_n'(x) + \frac{K_S h^2}{(EI)_C} \phi_m(x)\phi_n(x) \right] \mathrm{d}x = 0 \tag{16}
$$

From Eq. (16), it is easy to obtain that

$$
\int_0^L \left[\phi_n'''(x)\phi_m'''(x) + \frac{K_S h^2 (EI)_F}{(EI)_C (EI)_B} \phi_m''(x)\phi_n''(x) \right] \mathrm{d}x = 0 \tag{17}
$$

Eqs. (16) and (17) are, respectively, the orthogonality conditions about mass and stiffness for

the simply-supported composite beam.

Since the terms of $\phi_m(x)$ and $\phi_n(x)$ are asymmetric, and $c^* = 2\xi\omega m^*$, we have

$$\frac{\bar{c}}{(EI)_{\mathrm{B}}}\frac{\mathrm{d}\phi_n(x)}{\mathrm{d}x} = \frac{2\xi_n\omega_n\overline{m}}{(EI)_{\mathrm{B}}}\left[\frac{\mathrm{d}^2\phi_n(x)}{\mathrm{d}x^2} - \frac{K_{\mathrm{S}}h^2\phi_n(x)}{(EI)_{\mathrm{C}}}\right] \tag{18}$$

Likewise, by multiplying $\phi_m(x)$ to both sides of Eq. (18), and employing partial integral and the orthogonality conditions of Eqs. (16) and (17), we have

$$\frac{2\xi_n\omega_n\overline{m}}{(EI)_{\mathrm{B}}}\phi_m(x)\phi_n'(x)\Big|_0^L - \frac{\bar{c}}{(EI)_{\mathrm{B}}}\int_0^L \phi_n'(x)\phi_m(x)\mathrm{d}x = 0 \quad (m \neq n) \tag{19}$$

The orthogonality conditions of Eqs. (16), (17) and (19) provide the decoupling methods for the motion equation of composite beams, and can be conveniently applied in the derivation.

2.3 Buckling of the axially compressed beam

The simply supported sandwich beam is compressed by axial force F_0 (F_1 = 0, see Fig.1). The system of equilibrium Eqs. (12), (17), and (18) is approximately solved.

3. Vibration analysis of composite beams under moving load

3.1 Governing equation

Based on Eq. (11), (17)-(19), when for the governing equations all modes are superposed, we obtain

$$\begin{aligned}&\sum_{i=1}^{\infty}\left[\frac{\overline{m}}{(EI)_{\mathrm{B}}}\frac{\mathrm{d}^2\phi_i(x)}{\mathrm{d}x^2} - \frac{K_{\mathrm{S}}h^2\overline{m}\phi_i(x)}{(EI)_{\mathrm{C}}(EI)_{\mathrm{B}}}\right]\frac{\mathrm{d}^2q_i(t)}{\mathrm{d}t^2} + \sum_{i=1}^{\infty}\left[\frac{\bar{c}}{(EI)_{\mathrm{B}}}\frac{\mathrm{d}\phi_i(x)}{\mathrm{d}x}\right]\frac{\mathrm{d}q_i(t)}{\mathrm{d}t}\\ &+\sum_{i=1}^{\infty}\left[\frac{\mathrm{d}^6\phi_i(x)}{\mathrm{d}x^6} - \frac{K_{\mathrm{S}}h^2(EI)_{\mathrm{F}}}{(EI)_{\mathrm{C}}(EI)_{\mathrm{B}}}\frac{\mathrm{d}^4\phi_i(x)}{\mathrm{d}x^4}\right]q_n(t) = \left[\frac{1}{(EI)_{\mathrm{B}}}\frac{\partial^2 p(x,t)}{\partial x^2} - \frac{K_{\mathrm{S}}h^2 p(x,t)}{(EI)_{\mathrm{C}}(EI)_{\mathrm{B}}}\right]\end{aligned} \tag{20}$$

Utilizing the orthogonality relationships and the corresponding boundary conditions, Eq. (20) can be written as the following form

$$M_n^*\ddot{q}_n(t) + C_n^*\dot{q}_n(t) + K_n^*q_n(t) = P_n^*(t) \quad (n = 1, 2, 3\ldots\ldots) \tag{21}$$

Eq. (21) is the governing equation for a straight composite beam with uniform section, where M_n^*, C_n^*, K_n^* and P_n^* are the generalized mass, damping, stiffness and load, respectively, which can be expressed as

$$M_n^* = \frac{\overline{m}}{(EI)_{\mathrm{B}}}\int_0^L\left[\phi_n'(x)\phi_n'(x) + \frac{K_{\mathrm{S}}h^2}{(EI)_{\mathrm{C}}}\phi_n(x)\phi_n(x)\right]\mathrm{d}x \tag{22a}$$

$$C_n^* = \frac{2\xi_n \omega_n \overline{m}}{(EI)_B} \int_0^L \left[\phi_n'(x)\phi_n'(x) + \frac{K_S h^2}{(EI)_C} \phi_n(x)\phi_n(x) \right] \mathrm{d}x \tag{22b}$$

$$K_n^* = \int_0^L \left[\phi_n'''(x)\phi_n'''(x) + \frac{K_S h^2 (EI)_F}{(EI)_C (EI)_B} \phi_n''(x)\phi_n''(x) \right] \mathrm{d}x \tag{22c}$$

$$P_n^* = \frac{1}{(EI)_B} \int_0^L \left[\frac{K_S h^2 p(x,t)}{(EI)_C (EI)_B} - \frac{\partial^2 p(x,t)}{\partial x^2} \right] \phi_n(x) \mathrm{d}x \tag{22d}$$

2.2 Vibration equation of composite beams under moving load

Consider a simply-supported composite beam with uniform cross-section, where both $(EI)_F$ and $\overline{m}$ are constants, and load $P(t)$ moves on the beam at a speed V, as shown in Fig. 3.

For the moving load $P(t)$, the term P_n^* in Eq. (22) can be expressed as $\delta(x - Vt)P(t)$, where δ is the Dirac-delta function, it has the following features

$$\int_a^b \delta(x-\eta) f(x) \mathrm{d}x = \begin{cases} 0, & \eta < a < b \\ f(\eta), & a \le \eta \le b \\ 0, & a < b < \eta \end{cases} \tag{23a}$$

$$\int_a^b f(x) \frac{\mathrm{d}^n}{\mathrm{d}x^n} \delta(x-\eta) = (-1)^n \left[\frac{\mathrm{d}^n}{\mathrm{d}x^n} f(x) \right]_{x=\eta}, \quad a \le \eta \le b \tag{23b}$$

According to the derivation of Section 2.1, by substituting $\phi_n(x) = \sin(n\pi x / L)$ into Eq. (23), the specific expressions of all the generalized coefficients in the vibration equation are derived as follows

$$M_n^* = \frac{\overline{m}}{(EI)_B} \frac{L}{2} \left[\left(\frac{n\pi}{L} \right)^2 + \frac{K_S h^2}{(EI)_C} \right] \tag{24a}$$

$$C_n^* = \frac{2\xi_n \omega_n \overline{m}}{(EI)_B} \frac{L}{2} \left[\left(\frac{n\pi}{L} \right)^2 + \frac{K_S h^2}{(EI)_C} \right] \tag{24b}$$

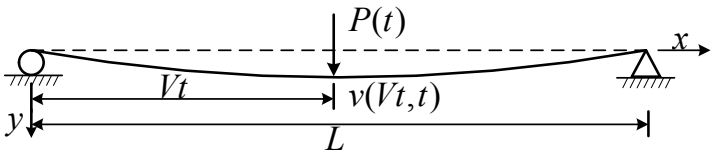

Fig. 3 Model of a composite beam subjected to a moving load

$$K_n^* = \frac{L}{2}\left(\frac{n\pi}{L}\right)^4\left[\left(\frac{n\pi}{L}\right)^2 + \frac{K_S h^2 (EI)_F}{(EI)_C (EI)_B}\right] \tag{24c}$$

$$\begin{aligned} P_n^* &= \frac{1}{(EI)_B}\int_0^L \delta(x-Vt)\left[\frac{K_S h^2 P(t)}{(EI)_C} - \frac{\partial^2 P(t)}{\partial x^2}\right]\phi_n(x)\mathrm{d}x \\ &= \begin{cases} \dfrac{P(t)}{(EI)_B}\left[\dfrac{(n\pi)^2}{L^2} + \dfrac{K_S h^2}{(EI)_C}\right]\sin\dfrac{n\pi Vt}{L}, & (0 \le t \le t_0) \\ 0, & (t \ge t_0) \end{cases} \end{aligned} \tag{24d}$$

where t_0 is the time of the load moving on the beam, i.e., L / V.

3.3 Solution to the vibration equation

Substituting M_n^*, C_n^*, K_n^* and P_n^* into Eq. (21), and divided by M_n^*, the normalized form of the n^{th} dynamic equilibrium equation for the simply-supported composite beams under moving load can be obtained as

$$\ddot{q}_n(t) + 2\xi_n\omega_n\dot{q}_n(t) + \omega_n q_n(t) = \frac{2P(t)}{m}\sin\frac{n\pi Vt}{L} \quad (n = 1, 2, \ldots\ldots) \tag{25}$$

where $m = \overline{m}L$ denotes the total mass of the beam.

Eq. (25) is a linear differential equation with constant coefficients, which has the same form with the conventional beams, merely the expression of M_n^*, C_n^*, K_n^* and P_n^* are more complicated. The response of each mode of the beam under moving load can be calculated with the Duhamel integral, and the ultimate physical response of the beam can be obtained by superposition of all modes concerned.

If the initial conditions of Eq. (25) are assumed as static, i.e., both $q_n(0)$ and $\dot{q}_n(0)$ are zero, the particular solution to the response can be written as

$$\begin{aligned} v(x,t) &= \sum_{n=1}^{\infty} q_n\phi_n(x) \\ &= 2m\sum_{n=1}^{\infty}\frac{(EI)_B\alpha}{\left[1+(n\pi)^2\alpha\right]}\frac{1}{\omega_{B,n}}\sin\frac{n\pi x}{L}\int_0^t P(t)\sin\frac{n\pi Vt}{L}e^{-\xi_n\omega_n(t-\tau)}\sin\omega_{D,n}(t-\tau)\mathrm{d}\tau \end{aligned} \tag{26}$$

where $\omega_{D,n}$ denotes the n^{th} circular frequency with damping. It is worth noticing that there is an additional coefficient in the right term compared to conventional beams.

Based on Eq. (26), the response of multiple loads moving on the composite beam at different speeds can be obtained easily. As for a concentrated load acting on a fixed position of the beam (i.e., $V = 0$), the dynamic response expression of the composite beam can be converted into series that matching summation conditions through a certain mathematical transformation, this will be discussed in another paper.

4. Case study

The simply-supported composite beam subjected to moving loads is studied to illustrate the application of the dynamic theory derived in this paper, and the results are compared with those from the model test.

4.1 Model test

The models have a span of 4200 mm, composed of a concrete slab and two steel girders. The concrete slab and steel girders are connected with headed studs as the shear connectors, whose diameter and height are 13 mm and 50 mm, respectively. There are two types of connection for the models: partial connection with shear connection degree 60% with 42 headed studs, which is expressed as PCB, and full connection with 70 headed studs, which is expressed as FCB. Detailed dimensions and structural layout can be found in Fig. 4. The definition of connectors' stiffness can be found in European Standard (2007) and the study of Gattesco (2009).

The 941B sensors and the corresponding data acquisition instrument (COINV) are used to measure the acceleration of the beams, and the displacement sensors to measure the vertical

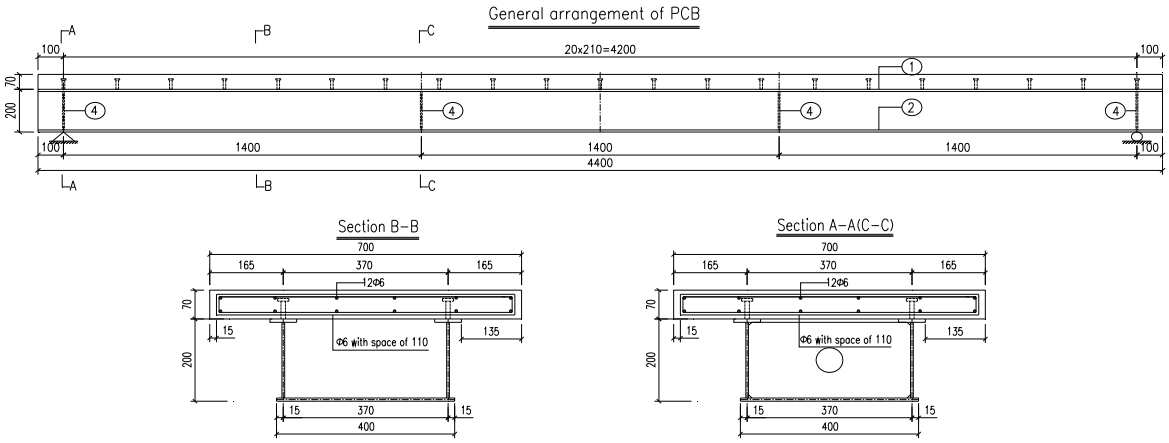

Fig. 4 Dimensions of the test beams (unit: mm)

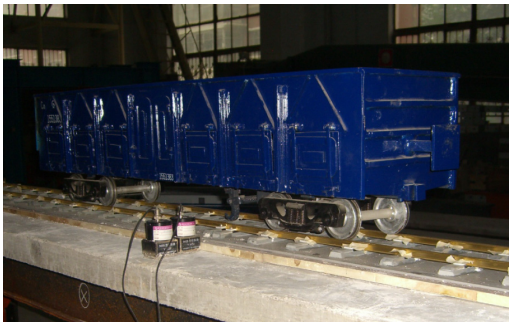

Fig. 5 Photograph of the model vehicle

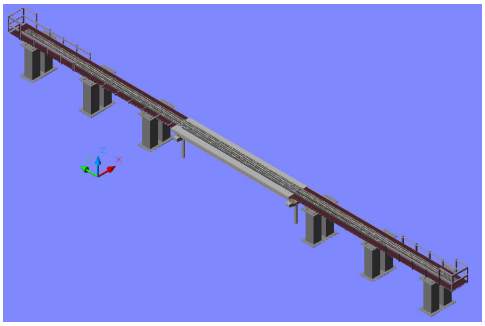

Fig. 6 Schematic diagram of the test platform

Table 1 Comparison of the 1st vertical natural frequencies of FCB and PCB (Hz)

Model	Theoretical value			γ_1^2	Numerical value		Test results
	K_S (MPa)	Slip	No slip		Slip	No slip	
FCB	305.32	22.546	28.91	0.608	25.93	31.607	23.13
PCB	183.19	20.921	28.91	0.517	24.11	31.208	21.16

displacement. A model vehicle with the scale of 1:10 based on the real train carriage of C70 in China is taken as the moving loads. The model vehicle has 2 bogies and 4 wheel-sets, and the self-weight is 62 kg. The model vehicle and the schematic diagram of test platform can be found in Figs. 5 and 6, respectively.

Compared in Table 1 are the theoretical, numerical and test results of the 1st vertical natural frequencies of the PCB and FCB beams. In the table, the theoretical ones are analyzed with Eq. (7), and the numerical ones are calculated by ANSYS. K_s is the longitudinal shear stiffness of unit length of the connector, and $K_s = \infty$ corresponds to the case without slip.

It can be seen from Table 1 that:

(1) The results considering relative slip are quite close to the test ones, while those without slip are 36.6% as much bigger, which validates the formulae conducted by this paper.
(2) The 1st vertical natural frequency decreases with the falling of shear connection degree, which shows that the relative slip decreased the global stiffness of the composite beams.
(3) Other details of dynamic characteristics for the model beams can be found in reference (Hou 2011).

4.2 Dynamic responses of composite beam under moving loads

4.2.1 Measured results from model test

Dynamic responses of the beam were measured when the vehicle travels through the beam at several speeds from 0.1 to 3.0 m/s.

In this test, the stiffness of the model beams (the 1st vertical frequencies are greater than 20 Hz) are relatively larger than the normal ones (the fundamental frequency is usually less than 10 Hz), and compared with the weight of the model beam, the moving loads are relatively lightweight, so the responses of the beams are not significant. This will lead to certain errors in the measured results produced by the irregularity of the track and other factors. To better compare with the calculated results, filtering of 80 Hz was conducted to remove the errors from the measured results. Shown in Fig. 7 are the measured acceleration and displacement time histories at midspan of the FCB beam under 62 kg model vehicle at speed of 2.35 m/s.

It can be seen that the acceleration of the beam excited by the model presents as an oscillation waveform and quickly attenuates with time, while in the displacement time history, a series peaks appear around the static deflection curve with a half-sinusoidal waveform. The measured maximum acceleration and displacement are 1.30 m/s^2 and 0.08 mm, respectively.

4.2.2 Numerical results and their comparison with measured ones

The numerical results are calculated according to Eq. (25), in which the 62-kg model vehicle is simplified as moving load series, as shown in Fig. 8. In the calculation, the damping ratio of the beam is taken as 0.02.

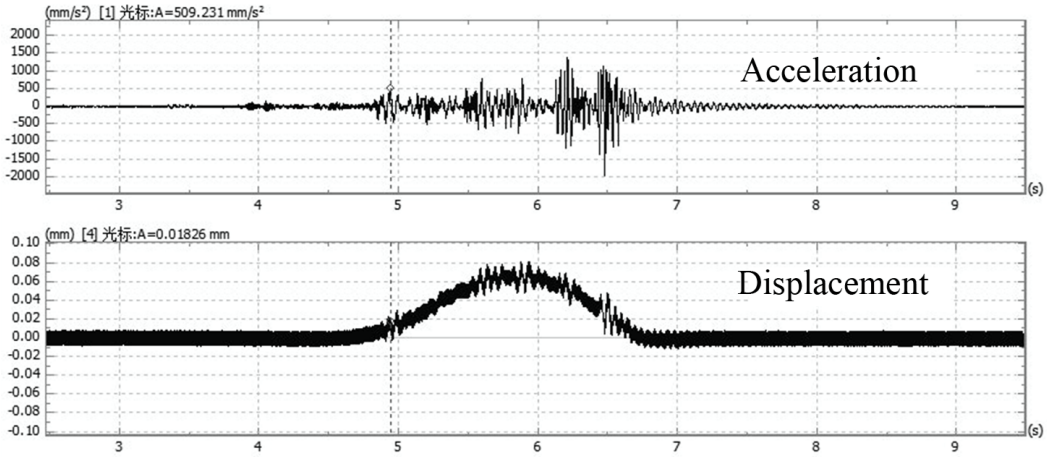

Fig. 7 Dynamic responses of FCB beam at midspan under 62 kg model vehicle

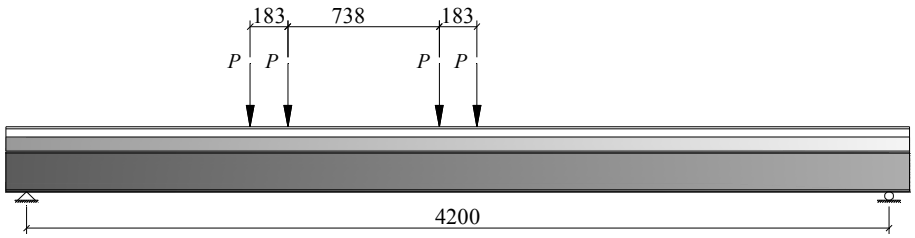

Fig. 8 Load series distribution of the model vehicle (mm)

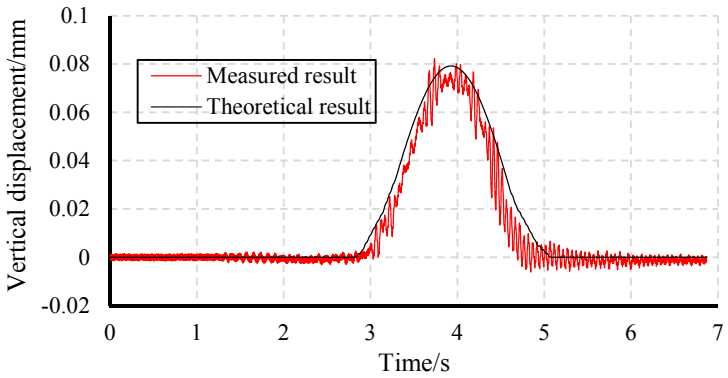

Fig. 9 Comparison of FCB under 62-kg vehicle between the test and theoretical results

Using the same parameters with the model test, the dynamic responses of the beam are calculated by the numerical model. Compared in Fig. 9 are the calculated and measured midspan time histories. On the whole, the calculated curve agrees well with the measured one. Since the influence of the track irregularity in the model test, there appear some higher frequency components in the measured curve.

Compared in Figs. 10 and 11 are the distributions of theoretical and measured maximum mid-span displacements of FCB and PCB under moving loads vs vehicle speed, and in Figs. 12 and 13 are the distributions of the corresponding dynamic factors.

These figures show that in the main trend, the theoretical results agree well with the measured ones, especially for the displacement of PCB and the dynamic factor of FCB. Within the scope of test speeds, the increase of midspan displacements and dynamic factors are not obvious with the speed, it is because of the higher stiffness of the model beams and relative lower speed of the model vehicle. Although there exist some errors between the calculated and the measured results, most of them are less than 5%, which shows the validity of the dynamic analysis theory proposed in this paper.

4.2.3 Influence of connection stiffness

To study the influence of shear connection stiffness, the dynamic responses of the beams are calculated. Shown in Fig. 14 are the calculated time histories for FCB and PCB with 62-kg vehicle at a speed of 10 m/s, in which the result of conventional beam (marked with CB, i.e., $K_S = \infty$, with other parameters unchanged) is also given.

The results show that under the same load and speed, the maximum displacements of PCB, FCB and CB at midspan are quite different, which are 0.094, 0.081 and 0.048 mm, respectively, showing that the greater the connection stiffness, the smaller the displacement of the beam.

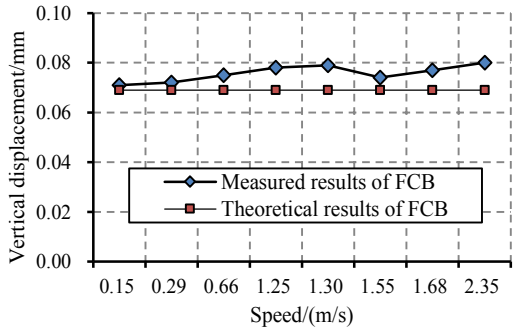

Fig. 10 Midspan displacement vs speed for FCB

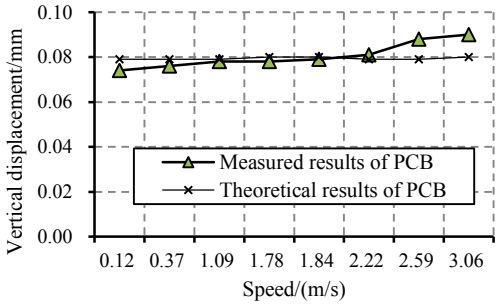

Fig. 11 Midspan displacement vs speed for PCB

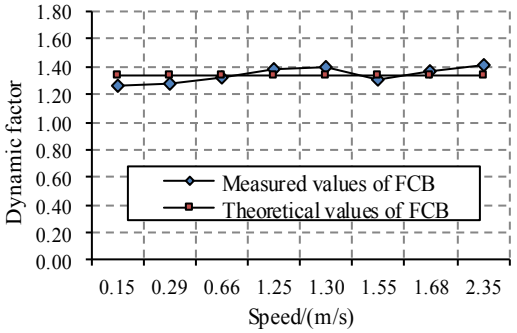

Fig. 12 Dynamic factor vs speed for FCB

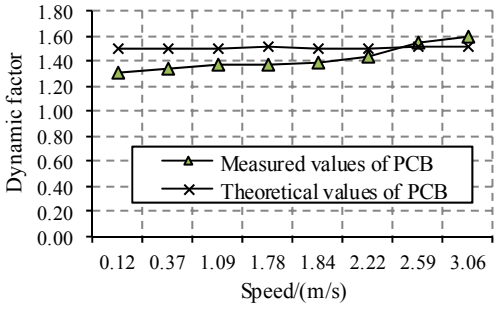

Fig. 13 Dynamic factor vs speed for PCB

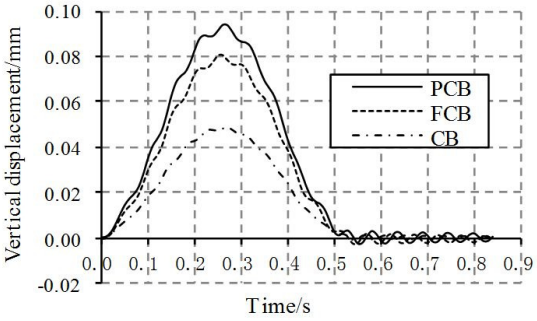

Fig. 14 Midspan displacement histories of the composite beam under model vehicle

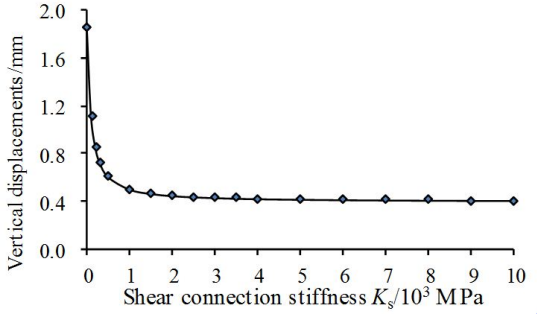

Fig. 15 Relationship between midspan displacement and shear connection stiffness K_s

Taking the PCB as an example, the relationship between the maximum displacement and shear connection stiffness K_s is shown in Fig. 15, where the weight and speed of the vehicle are fixed to 500 kg and 50 m/s, respectively, while the other parameters keep unchanged.

Together by analysis of Eq. (7), the displacement response of the composite beam under moving loads, it can be found from Fig. 15 that

(1) When K_s approaches to 0, the displacement of PCB reaches to the maximum value, i.e. about 1.865 mm. This means that the concrete slab and steel girder have lost their shear connection, and just simply overlapped.
(2) With the increase of K_s, the displacement of composite beam decreases rapidly. For K_s higher than 500 MPa (about 6 times of FCB) or 300 MPa (10 time of PCB, the connection degree is about 60%), the displacement gradually becomes a fixed value, which is 0.4 mm.
(3) The shape of the curve is not correlated to the vehicle parameters such as speed and weight, but related to the geometric dimension and material characteristics of the beam.
(4) The ratio between the maximum and minimum displacements is 4.567, which is related to the sectional characteristics of the composite beam.

Presented in Fig. 16 are the $\alpha - \gamma_n^2$ curves, which illustrates the relationship between the shear connection stiffness and the stiffness reduction factor of the composite beam.

It is interesting to notice that both the relationships and differences exist between Figs. 16 and 15, the former shows the relationship between the dynamic stiffness of each order and shear connection stiffness, and the latter shows the relationship between the global stiffness of the

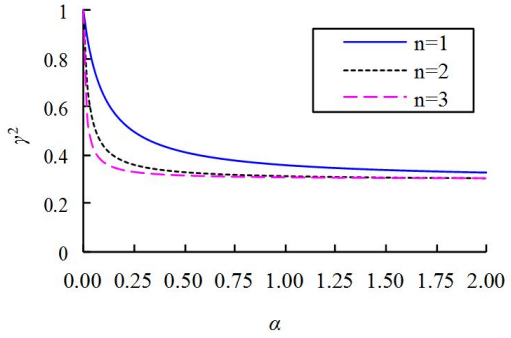

Fig. 16 Relationship curves of $\alpha - \gamma_n^2$

composite beam and shear connection stiffness, which is the weighted results of the dynamic stiffness of all orders considered.

The above analyses show that the dynamic parameters of the composite beams, such as natural frequency, acceleration and displacement, are significantly influenced by the shear connection stiffness (reflected with DSRF and FRF), which behave as follows:

(1) The DSRF and FRF of the composite beam have definite expressions. They both decrease with the shear connection stiffness, and converge to a certain constant (the maximum value is 1), which is related to the sectional parameters of the beam but not the characteristics of the shear connector.
(2) Both the DSRF and FRF decrease rapidly with the natural frequency order considered, and DSRF decreases more significantly than FRF. When the modal superposition method is adopted, the higher the order considered, the more accuracy of the calculation result can be obtained, despite there is less and less contribution of higher orders to the final calculation result.

5. Conclusions

Based on the fundamental dynamic theory of composite beams founded by this paper, the dynamic responses of composite beams under moving loads are derived, and the theoretical results show good agreement with the test ones.

The main conclusions are as follows:

(1) The motion equation of the composite beam becomes complicated when the relative slip between concrete slab and steel girder is taken into account, which explicitly reflects the influence of shear connectors.
(2) The vertical natural frequencies of the composite beam decrease obviously when the interface slip is considered, which shows great influence on the global stiffness. Consequently, such influence ought to be taken into account not only in static but also in dynamic calculation.
(3) The influences of shear connection stiffness cannot be ignored if the interface slip is involved, which should be considered not only in the static but also dynamic calculation,

and should be paid more attention in calculation, design and experiment, or else considerable deviation is inevitable.

(4) In dynamic calculation of composite beams, the stiffness should not be reduced as the same factor to all orders, but as different ones according to the expression of the dynamic stiffness reduction factor (DSRF), which is related to the sectional parameters of the beam but not the characteristics of the shear connector, and varies with the order of the natural vibration characteristic.

Acknowledgments

This study is sponsored by the State Fundamental Research Funds "973" Program (2013CB036203), the Natural Science Foundation (51178025), the "111" Project (B13002), the Fundamental Research Funds for the Central Universities (2013JBM011) of China, and Key Topics of Science and Technology Research Project for Colleges and Universities of Hebei Province (ZD2014025).

References

Andrews, E.S. (1912), *Elementary Principles of Reinforced Concrete Construction*, Scott, Greenwood and Son, London, UK.

Banerjee, J.R. (2001), "Frequency equation and mode shape formulae for composite Timoshenko beams", *Compos. Struct.*, **51**(4), 381-388.

Biscontin, G., Morassi, A. and Wendel, P. (2000), "Vibrations of steel-concrete composite beams", *J. Vib. Control*, **6**(5), 691-714.

Dilena, M. and Morassi, A. (2003), "A damage analysis of steel-concrete composite beams via dynamic methods: Part II. Analytical models and damage detection", *J. Vib. Control*, **9**(5), 529-565.

Esmailzadeh, E. and Jalili, N. (2003), "Vehicle-passenger-structure interaction of uniform bridges traversed by moving vehicles". *J. Sound Vib.*, **260**(4), 611-635.

European Standard (2007), Design of composite steel and concrete structures, Part 1.1: General rules and rules for buildings-General rules, EN 1994-1-1, Eurocode 4.

Galambos, T.V. (2000), "Recent research and design developments in steel and composite steel-concrete structures in USA", *J. Constr. Steel. Res.*, **55**(1/3), 289-303.

Gattesco, N. (1999), "Analytical modeling of nonlinear behavior of composite beams with deformable connection", *J. Constr. Steel. Res.*, **52**(2), 195-218.

Girhammar, U.A., Pan, D.H. and Gustafsson, A. (2009). "Exact dynamic analysis of composite beams with partial interaction", *Int. J. Mech. Sci.*, **51**(8), 565-582.

Hou, Z.M., Xia, H., Li, Y.S. and Dai, Y.L. (2011), "Dynamic response analysis and shear stud damage identification of steel-concrete composite beams", *Proceedings of the 14th Asia Pacific Vibration Conference*, Hong Kong, December, pp. 1711-1720.

Hou, Z.M., Xia, H. and Zhang, Y.L. (2012), "Dynamic analysis and shear connector damage identification of steel-concrete composite beams", *Steel Compos. Struct., Int. J.*, **13**(4), 327-341.

Huang, C.W. and Su, Y.H. (2008), "Dynamic characteristics of partial composite beams", *Int. J. Struct. Stab. Dy.*, **8**(4), 665-685.

Jiang, L.Z., Ding, F.X. and Yu, Z.W. (2006), "Experimental study on the integrated dynamic behavior of continuous steel-concrete composite girders of railway bridges", *Chinese Railway. Sci.*, **27**(5), 60-65. [In Chinese)

Kim, N. (2009), "Dynamic stiffness matrix of composite box beams", *Steel Compos. Struct., Int. J.*, **9**(5),

473-497.
Kroflic, A., Planinc, I., Saje, M. and Cas, B. (2010), "Analytical solution of two-layer beam including interlayer slip and uplift", *Struct. Eng. Mech., Int. J.*, **34**(6), 667-683.
Nie, J.G. and Cai, C.S. (2003), "Steel-concrete composite beams considering shear slip effects", *J. Stru. Eng., ASCE*, **129**(4), 495-506.
Nie, J.G., Shen, J.M. and Yuan, Y.S. (1994), "A general formula for predicting the deflection of simply supported composite steel concrete beams with the consideration of slip effect", *Eng. Mech.*, **11**(1), 21-27.
Nie, J.G., Li, Y., Yu, Z.W. and Chen, Y.Y. (1998), "Study on short and long-term rigidity of composite steel-concrete beams", *J. Tsinghua Univ.* (*Sci & Tech*), **38**(10), 38-41.
Ranzi, G. and Zonab, A. (2007), "A steel–concrete composite beam model with partial interaction including the shear deformability of the steel component", *Eng. Struct.*, **29**(11), 3026-3041.
Taly, N. (1998), *Design of Modern Highway Bridges*, McGraw-Hill Companies Inc., New York, NY, USA.
Wang, Y.C. (1998), "Deflection of steel-concrete composite beams with partial shear interaction", *J. Struct. Eng.*, **124**(10), 1159-1265.
Wang, J.Q., Lü, Z.T. and Liu, Z. (2005), "Consistency factor method for calculating deformation of composite steel-concrete girders with partial shear connection", *J. Southeast Univ.*, **35**(Sup (I)), 5-10.
Won, S.G., Bae, S.H., Jeong, W.B., Cho, J.R. and Bae, S.R. (2012), "Forced vibration analysis of damped beam structures with composite cross-section using Timoshenko beam element", *Struct. Eng. Mech., Int. J.*, **43**(1), 15-30.
Xia, H., Zhang, N. and De Roeck, G. (2003), "Dynamic analysis of high speed railway bridge under articulated trains", *Comput. Struct.*, **81**(26-27), 2467-2478.
Xia, H., Xu, Y.L., Chan, T.H.T. and Zakeri, J.A. (2007), "Dynamic responses of railway suspension bridges under moving train", *Sci. Iran.*, **14**(5), 385-394.
Xu, R.Q. and Wu, Y.F. (2007), "Static, dynamic, and buckling analysis of partial interaction composite members using Timoshenko's beam theory". *Int. J. Mech. Sci.*, **49**(10), 1139-1155.
Zhang, Y.Z. (2002), "Analysis on responses of continuous composite beams in high-speed railways". *J. Chin. Railway. Soc.*, **24**(6), 84-88.
Zhang, Y.L. (2009), "Theoretical analysis and experimental research on behavior and crack control of negative moment zone in steel-concrete composite beams", Doctoral Dissertation, Beijing Jiaotong University, China, 20-32. [In Chinese]

CC